

Materials made available here are subject to the IEEE copyright policy. Find policy here:
<http://iee.org>

By choosing to view this document, you agree to fulfill all of your obligations with respect to IEEE-copyrighted material.

The publication can be found at the following URL on the IEEE website:
http://ieeexplore.ieee.org/xpl/freeabs_all.jsp?arnumber=1174027

Coherence-Multiplexed Fiber-Optic Sensor Systems for Measurements of Pressure and Temperature Changes

W. J. Bock, M. S. Nawrocka, and W. Urbanczyk

Abstract—A digital demodulation method for read-out of phase changes induced in coherence-multiplexed sensors based on highly birefringent fibers is described. The method employs the fringe counting principle and enables registration of the phase shifts simultaneously induced in two multiplexed sensors with a maximum frequency of 10 kHz and resolution of 1/4 of the interference fringe. The performance of three multiplexed systems interrogated using the proposed detection method is investigated. The first system is composed of two serial multiplexed sensors serving for measurements of pressure and temperature changes in the same location, while the two other systems are composed of two parallel or serial multiplexed temperature-compensated sensors serving for pressure measurements at different locations.

Index Terms—Coherence-multiplexing, demodulation method, fiber-optic sensor, pressure and temperature measurements.

I. INTRODUCTION

THERE are many sensors that simultaneously control various static and dynamic changes in different measurands including pressure, temperature, strain, and elongation [1]–[3]. However, the problem of simultaneously measuring dynamic changes of two physical parameters has not been explored so far. In this paper we present three coherence-multiplexed systems of interferometric sensors based on highly birefringent fibers for simultaneous measurement of two parameters. The first investigated system is composed of two serial multiplexed sensors, which can be used for measurements of temperature and pressure changes at the same location. In this case, as sensing elements we used side-hole and bow-tie fibers. They are spliced together with rotation of their polarization axes by an angle that assures the highest possible contrast for the interference signals associated with the bow-tie fiber itself and for the differential pattern produced by the two fibers.

The other two systems are composed of two hydrostatic pressure sensors compensated for temperature, which are arranged in parallel or serial configuration. These systems can be used for measuring pressure changes at two different locations. Tem-

perature compensation of the multiplexed sensors is achieved by using the side-hole fiber and elliptical core fiber of appropriate lengths, which are spliced with rotation of their polarization axes by 90°.

Since highly birefringent fibers are sensitive to both pressure and temperature, fiber-optic pressure sensors based on this type of fiber have to be compensated for temperature. Most often, a reference fiber located as close as possible to the sensing fiber is used to assure temperature compensation [4]. In such a configuration, hydrostatic pressure has access only to the sensing element. This method of compensation is not very suitable in sensors measuring fast pressure changes, which always induce temperature gradients between the sensing and the reference fibers. The sensors described in this paper are based on the side-hole fiber, which shows high and negative sensitivity to hydrostatic pressure. This specific feature of the side-hole fiber enabled us to propose a novel sensor construction, in which the sensing and compensating elements are located in the same compartment of the sensor housing. This temperature compensation method is better suited for measurements of fast pressure changes than other known solutions.

It is worth mentioning that the concept of simultaneous measurement of quasistatic changes of pressure and temperature using intermodal interference between x - and y -polarized LP_{01} and LP_{11} modes combined with a polarimetric detection scheme was earlier analyzed in [1]. The limitations of the sensing method described in [1] are associated with small differences in sensitivities to temperature and pressure for LP_{01} and LP_{11} modes, which result in limited resolution in recovering these two parameters. Furthermore, the polarimetric detection method used in [1] requires highly coherent light, which excludes coherency multiplexing of such sensors. The two-parameter systems proposed in this paper overcome the main limitations of the idea reported in [1].

II. SYSTEM FOR MEASUREMENTS OF SIMULTANEOUS TEMPERATURE AND PRESSURE CHANGES AT THE SAME LOCATION

The proposed system for simultaneous measurements of pressure and temperature changes employs the coherency addressing principle [5]. Such systems are composed of sensing and decoding interferometers with matched optical path delays. In our case the sensing interferometers are two pieces of highly birefringent fiber of different types (bow-tie and side-hole) while crystalline-quartz plates with analyzers are used as the

Manuscript received May 29, 2001; revised July 17, 2002. This work was supported by the Natural Sciences and Engineering Research Council of Canada, by the FCAR of Quebec, Canada, and by the Polish Committee for Scientific Research.

W. J. Bock is with the Laboratoire d'Optoélectronique, Département d'Informatique, Université du Québec à Hull, Hull, QC J8X 3X7, Canada (e-mail: bock@uqah.quebec.ca).

M. S. Nawrocka and W. Urbanczyk are with the Institute of Physics, Wrocław University of Technology, Wrocław, Poland (e-mail: urban@rainbow.if.pwr.wroc.pl).

Digital Object Identifier 10.1109/TIM.2002.806034

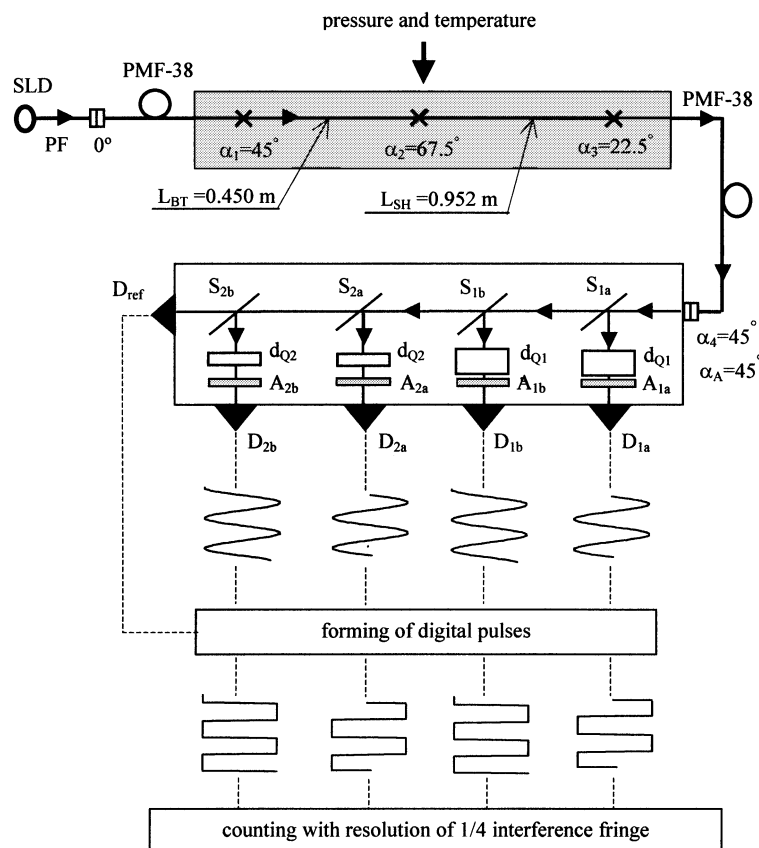


Fig. 1. Configuration of the system of two serial multiplexed sensors for hydrostatic pressure and temperature measurements: SLD—superluminescent diode; PF—polarizing fiber; S_{1a} , S_{1b} , S_{2a} , and S_{2b} —beam splitters; d_{Q1} , d_{Q2} —crystalline-quartz delay plates; A_{1a} , A_{1b} , A_{2a} , and A_{2b} —analyzers; D_{1a} , D_{1b} , D_{2a} , D_{2b} , and D_{ref} —pin photodiodes.

decoding interferometers, as shown in Fig. 1. The system is powered by a superluminescent diode pigtailed with 3M polarizing fiber ($\lambda_0 = 830$ nm, $\Delta\lambda = 25$ nm, $P = 0.2$ mW). Linearly polarized light from the polarizing fiber is coupled by a polarization maintaining connector into one mode of the linking fiber (Corning PMF-38). The linking fiber and the active part of the sensor are spliced to each other with rotation of their polarization axes by $\alpha_1 = 45^\circ$. Therefore, two polarization modes are excited in the first active element of the sensor (bow-tie fiber, 0.450 m long). The second active element is the side-hole fiber (0.952 m long), which is spliced with the bow-tie fiber with rotation of their polarization axes by $\alpha_2 = 67.5^\circ$. The lead-out fiber is spliced to the side-hole fiber with rotation of their polarization axes by $\alpha_3 = 22.5^\circ$. Such alignment assures the highest possible visibility at the center of the interference pattern associated with the bow-tie fiber itself ($V_{BT} = 0.25$) and also at the center of the differential pattern produced by the bow-tie and the side-hole fibers ($V_{SH-BT} = 0.3$). The side-hole fiber is highly sensitive to pressure $K_{SH}^P = -94$ rad/MPa m and has low sensitivity to temperature $K_{SH}^T = -0.47$ rad/K m, compared to other fibers known from the literature. The sensitivities of the bow-tie fiber to pressure and temperature are equal to $K_{BT}^P = +7.9$ rad/MPa m and $K_{BT}^T = -4.4$ rad/K m, respectively. The bow-tie and side-hole fibers are wound on a coil 7 cm in diameter and placed in a steel housing. Such a configuration diminishes the sensor size and makes it more suited for practical applications.

The first interference signals associated with the bow-tie fiber are decoded in the first two detection channels. To balance the optical path delay (OPD) introduced by the bow-tie fiber we placed the quartz compensating plates with a thickness of $d_{Q1} = 20$ mm in these channels. By tilting the plates we shifted these two signals in phase by 90° , thereby assuring unambiguous fringe counting with a resolution of $1/4$ of an interference fringe. The differential interference signals are registered in the third and fourth detection channels, in which two quartz retardation plates with a thickness $d_{Q2} = 4$ mm are placed, again tilted to introduce the phase shift of 90° . Due to the high sensitivity to pressure of the side-hole fiber, the phase shift in the differential signal induced by a pressure change of 1 MPa is much higher than that induced by a temperature change of 1°C . At the same time, the phase shifts induced in the bow-tie fiber itself by the unit change of both measurands are almost equal to each other.

It is possible to simultaneously measure the phase shifts induced by pressure and temperature changes in the two interference signals by converting sinusoidal intensity changes into digital pulses shifted in phase by 90° . The maximum counting frequency in the considered set-up is limited to 10 kHz by the speed of the computer board. The information about changes of pressure Δp and temperature ΔT may be retrieved by solving the following set of equations:

$$\begin{bmatrix} \Delta\phi_{BT}(p, T) \\ \Delta\phi_{SH-BT}(p, T) \end{bmatrix} = \begin{bmatrix} S_{BT}^P & S_{BT}^T \\ S_{SH-BT}^P & S_{SH-BT}^T \end{bmatrix} \begin{bmatrix} \Delta p \\ \Delta T \end{bmatrix} \quad (1)$$

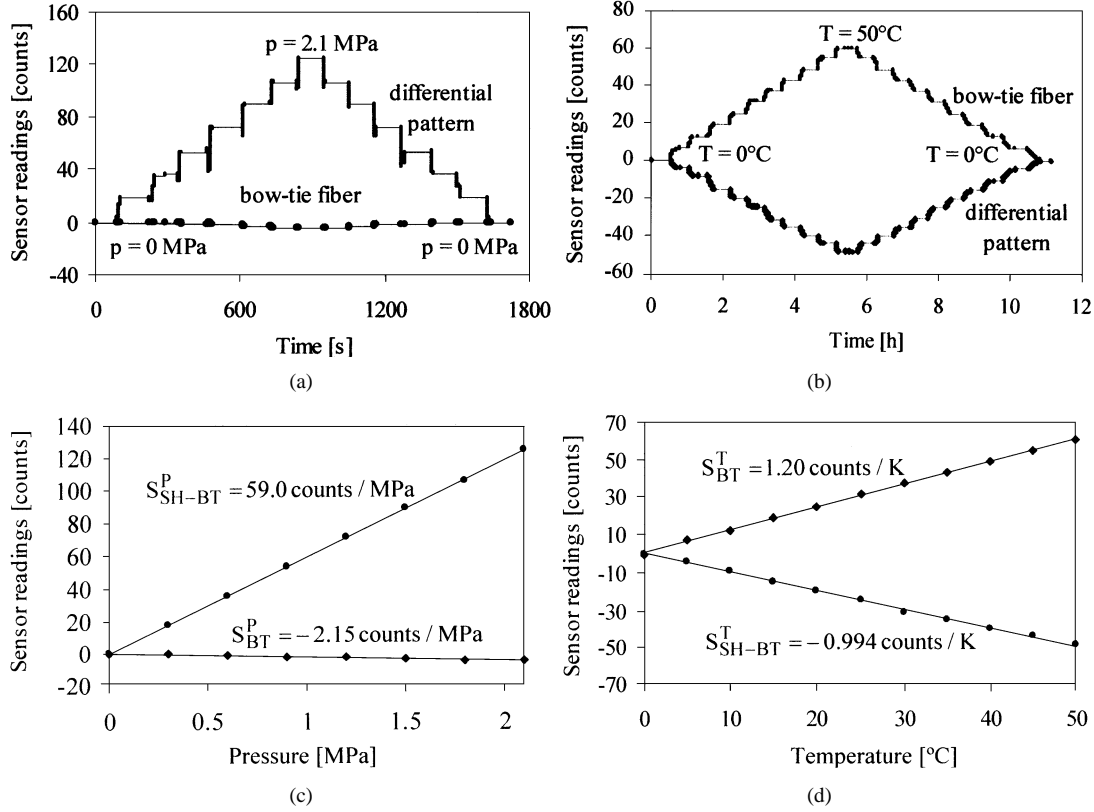


Fig. 2. System response to pressure changes in the range (a) from 0 to 2.1 MPa with a step of 0.3 MPa and to (b) temperature changes from 0 to 50 °C with a step of 5 °C. The sensitivity coefficients were calculated using calibration curves shown in (c) and (d).

where $\Delta\phi_{BT}(p, T)$ is the phase shift introduced by the bow-tie fiber and $\Delta\phi_{BT-SH}(p, T)$ is the differential phase shift introduced by the bow-tie and side-hole fibers, both expressed in number of digital pulses. The sensitivities of the respective interference signals to pressure and temperature are related to the sensor construction and may be represented by the following equations:

$$S_{BT}^P = K_{BT}^P L_{BT} \quad (2)$$

$$S_{BT}^T = K_{BT}^T L_{BT} \quad (3)$$

$$S_{SH-BT}^P = K_{SH}^P L_{SH} - K_{BT}^P L_{BT} \quad (4)$$

$$S_{SH-BT}^T = K_{SH}^T L_{SH} - K_{BT}^T L_{BT}. \quad (5)$$

In order to determine the sensitivity coefficients, we calibrated the system for quasistatic pressure and temperature changes. The calibration results shown in Fig. 2 allowed us to calculate the elements of the sensitivity matrix S_{BT}^P , S_{BT}^T , S_{SH-BT}^P , and S_{SH-BT}^T . In the differential pattern produced by the bow-tie and side-hole fiber, the pressure and temperature sensitivities are equal to $S_{SH-BT}^P = 59.0 \text{ counts/MPa}$ (92.6 rad/MPa) and $S_{SH-BT}^T = -0.994 \text{ counts/K}$ (-1.56 rad/K), respectively. For the pattern produced by the bow-tie fiber the sensitivities are equal to $S_{BT}^P = -2.15 \text{ counts/MPa}$ (-3.37 rad/MPa) and $S_{BT}^T = 1.20 \text{ counts/K}$ (1.89 rad/K), respectively.

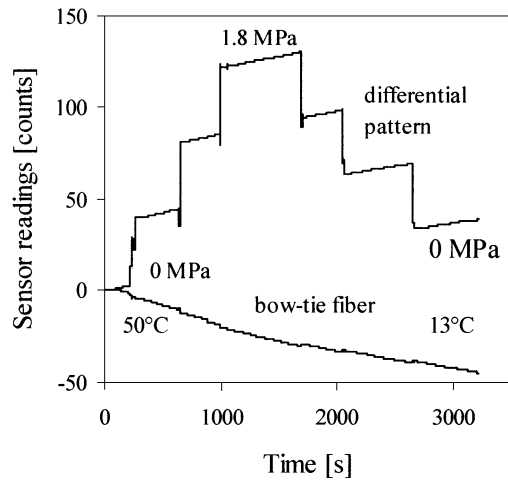
Knowing the sensitivity matrix it is possible to solve the set of equations (1) and to determine changes in the two parameters. The reconstruction procedure is illustrated in Fig. 3. It shows the system response to simultaneous changes of pressure

and temperature, as well as reconstructed values of the two parameters. In this test the pressure was increased from 0 MPa to 1.8 MPa with a step of 0.6 MPa, while at the same time the temperature was decreased continuously from 50 °C to 13 °C. The maximum difference between the calculated and the actual value of pressure and temperature change is equal to 0.02 MPa and 1 °C, respectively, which in both cases corresponds to 1% of the sensor full scale. The overall precision of measurements is limited mainly by the uncertainties in determining the sensitivity coefficients in equation (1), which affect the precision of recovering temperature and pressure after matrix inversion.

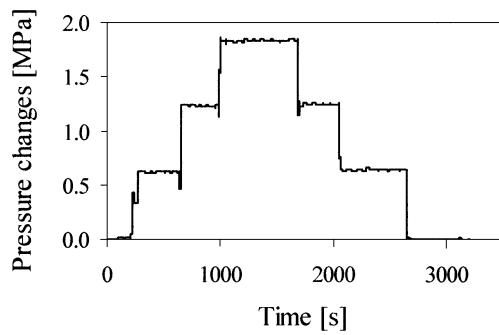
III. PARALLEL AND SERIAL MULTIPLEXED SENSOR SYSTEMS FOR MEASUREMENTS OF PRESSURE CHANGES AT DIFFERENT LOCATIONS

The construction details of both multiplexed systems composed of two hydrostatic pressure sensors are shown in Fig. 4. The sensing part in each sensor consists of the side-hole fiber and elliptical core fiber spliced with rotation of their polarization axes by 90°. In a parallel multiplexed system [Fig. 4(a)], the highly birefringent leading-out fibers are connected through polarization maintaining connectors (PMC) to the inputs of a Y-type polarization maintaining coupler. The output of the coupler is connected to the detection unit shown in Fig. 1.

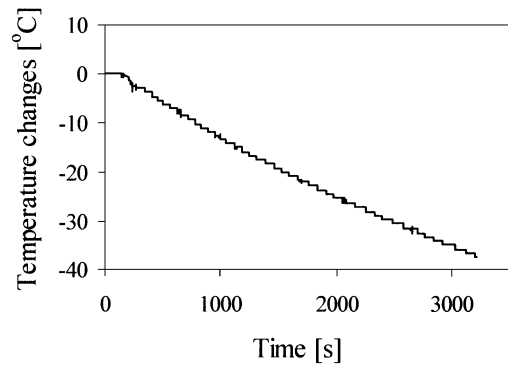
In a serial multiplexed system the two sensors are connected with 3M polarizing fiber (PF) aligned at an angle of 0° with respect to the leading fibers [Fig. 4(b)]. Such alignment of the polarizing fiber assures maximum contrast (equal to 0.5) of the interference signals associated with individual sensors [5].



(a)



(b)



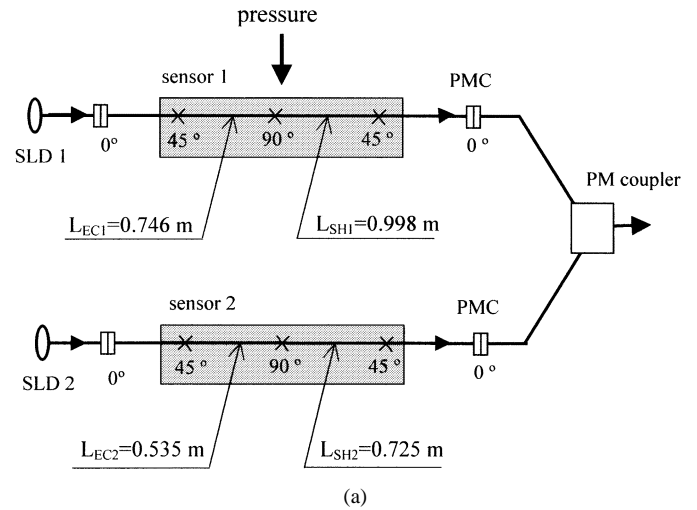
(c)

Fig. 3. (a) System response to simultaneous changes of pressure and temperature and (b) reconstructed values of pressure and (c) temperature. Pressure was increased from 0 MPa to 1.8 MPa with a step of 0.6 MPa while at the same time temperature was decreased continuously from 50 °C to 13 °C.

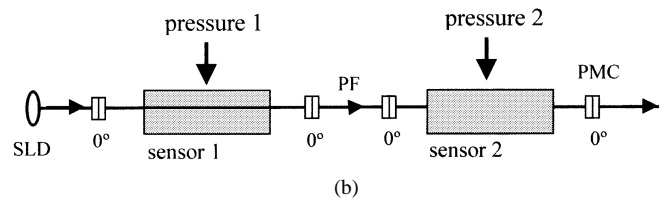
The coherency addressing principle requires that the OPD introduced by the first sensor be compensated by quartz plates 20 mm in thickness, while the OPD introduced by the second sensor is compensated by 4 mm quartz plates. This is equivalent to the following conditions:

$$\Delta N_{SH_i} L_{SH_i} - \Delta N_{EC_i} L_{EC_i} = \Delta N_Q d_{Q_i}, \quad \text{for } i = 1 \text{ or } 2 \quad (6)$$

where ΔN_{EC} , ΔN_{SH} , is the group birefringence of elliptical core and side-hole fibers respectively, while ΔN_Q and d_Q are the group birefringence and the thickness of the compensating quartz plates, respectively. The lengths L_{SH} and L_{EC} have to be inversely proportional to the temperature sensitivities of the



(a)



(b)

Fig. 4. System of two (a) parallel and (b) serial multiplexed sensors for hydrostatic pressure measurements. Both sensors are compensated for temperature changes.

respective fibers in order to compensate temperature-induced phase shifts in the two sensing elements

$$\frac{K_{EC_i}^T}{K_{SH_i}^T} = \frac{L_{SH_i}}{L_{EC_i}} \quad \text{for } i = 1, 2. \quad (7)$$

To fulfill simultaneously the conditions (6) and (7) in both sensors, we used the elliptical core and side-hole fiber of different types in each sensor. It should be noted that the pressure-induced phase changes in the two fibers add to each other. This is because the signs of pressure sensitivity in the side-hole and elliptical core fiber are opposite. This specific feature of the side-hole fiber makes it possible to locate the sensing and compensating fibers in the same chamber of the sensor housing. Such a construction of the sensor is more suited for compensating temperature effects associated with fast compression/decompression processes than the classical compensation configuration, in which pressure acts only on one fiber. Fast pressure changes always cause temperature changes and thus induce temperature differences between the sensing and the compensating elements, if they are located at different places.

The performance of the two systems was investigated in several temperature and pressure tests. Both sensors were calibrated for quasistatic pressure changes using the Harwood DWT-35 pressure generator with a precision of 0.1% as a reference. The results of calibration carried out for the parallel configuration are shown in Fig. 5(a). The number of counts registered by a computer was plotted versus applied pressure, in the range from 0 to 3.6 MPa, with a step of 0.6 MPa. The calibration procedure allowed us to determine the sensors' sensitivities to pressure, which are equal to 75.0 counts/MPa (117.8 rad/MPa) and 40.5 counts/MPa (63.7 rad/MPa), respectively, for the first and the second sensor. In Fig. 5(b) we also show the response of two

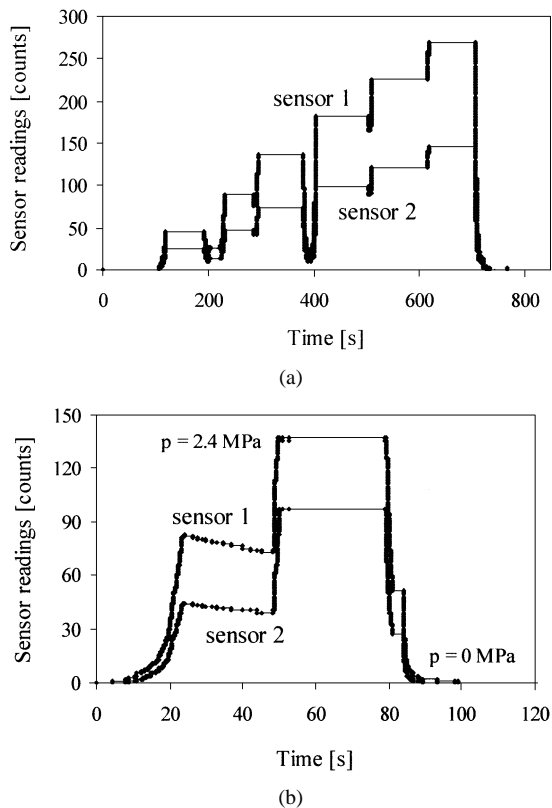


Fig. 5. Calibration of parallel multiplexed sensors using (a) quasistatic pressure changes from 0 MPa to 3.6 MPa with a step of 0.6 MPa and (b) response of two other sensors arranged in serial configuration to pressure changes from 0 MPa to 2.4 MPa.

other sensors arranged in serial configuration to the pressure changes from 0 MPa to 2.4 MPa.

The sensors' temperature stability was also tested at different pressures using the Haake C temperature stabilizer with a precision of 0.1 °C. Both sensors showed a residual response to temperature of the order of one count in the temperature range from 10 °C to 50 °C, which corresponds to 0.5% of the sensor's FS. This small but nonzero effect was most probably associated with a difference in second-order sensitivities (dependence of temperature sensitivity upon pressure) in the side-hole and elliptical core fibers and with the technological limits to which the lengths L_{SH} and L_{EC} can be controlled (± 2 mm).

IV. SUMMARY

We presented three coherence-multiplexed fiber-optic systems based on highly birefringent fibers. The first proposed system of two serial multiplexed sensors may be used in simultaneous measurements of pressure and temperature changes at the measurement location, while the two other systems composed of parallel or serial multiplexed temperature-compensated sensors may be used in measurements of hydrostatic pressure changes at different locations. In each

case the side-hole fiber was employed as one of the sensing elements, which assured high sensitivity to pressure of the tested sensors.

Furthermore, in the case of the temperature-compensated sensors, the negative sign of the pressure sensitivity of the side-hole fiber allowed us to mount the sensing and compensating fibers in the same compartment of the sensor head. This prevents temperature gradients between the two elements and makes the sensor almost insensitive to temperature changes.

The measurement range of the tested sensors can be modified by changing the lengths of the sensing elements. Furthermore, the maximum counting frequency, now equal to 10 kHz, can be further increased by applying a faster computer board and faster pin photodiodes. The sensor systems described in this paper will be applied in civil engineering to monitor vibrations of large constructions using specially developed hydraulic pads integrated with fiber-optic pressure sensors, which serve as the load-pressure transducers. This technology has already been employed to monitor quasistatic loads [6], [7].

REFERENCES

- [1] W. J. Bock and T. A. Eftimov, "Simultaneous hydrostatic pressure and temperature measurement employing an LP_{01} - LP_{11} fiber-optic polarization-sensitive intermodal interferometer," *IEEE Trans. Instrum. Meas.*, vol. 43, pp. 337-340, 1994.
- [2] K. T. V. Grattan and B. T. Meggitt, *Optical Fiber Sensor Technology*. London, U.K.: Chapman & Hall, 1995.
- [3] N. Furstenau, M. Schmidt, W. J. Bock, and W. Urbanczyk, "Dynamic sensing with a fiber-optic polarimetric pressure transducer with two-wavelength passive quadrature readout," *Appl. Opt.*, vol. 37, pp. 663-671, 1998.
- [4] J. P. Dakin and C. A. Wade, "Compensated polarimetric sensor using polarization-maintaining fiber in a differential configuration," *Electron. Lett.*, vol. 20, pp. 51-53, 1984.
- [5] A. W. Wozniak, P. Kurzynowski, W. Urbanczyk, and W. J. Bock, "Contrast analysis for a fiber-optic white-light interferometric system," *Appl. Opt.*, vol. 36, pp. 8862-8870, 1997.
- [6] W. J. Bock, W. Urbanczyk, T. A. Eftimov, and J. Chen, "Development and performance of fiber optic sensor systems for absolute and quasistatic measurements in civil engineering applications," in *Proc. Int. Conf. Applicat. Photon. Technol.*, Montréal, Canada, July 29-Aug. 1, 1996.
- [7] —, "Development and performance of fiber optic sensor systems for absolute and quasistatic measurements in civil engineering applications," in *Proc. Int. Conf. Applicat. Photon. Technol.*, G. A. Lampropoulos and R. A. Lessard, Eds. New York: Plenum, 1997, pp. 723-729.

W. J. Bock, photograph and biography not available at the time of publication.

M. S. Nawrocka, photograph and biography not available at the time of publication.

W. Urbanczyk, photograph and biography not available at the time of publication.